(NSERC) of Canada (Ottawa), the Formation de Chercheurs et d'Action Concertée (Quebec), and the North Atlantic Treaty Organization (No. 046.81); work at Brookhaven National Laboratory was done under contract with the U.S. Department of Energy and supported by its Office of Basic Energy Sciences. N.S. is grateful to NSERC (Ottawa) for a generous grant for the Canadian Picosecond Laser Laboratory at Concordia University.

Registry No. $Os(OEP)(py)_2$, 51286-87-4; $Os(OEP)(NO)_2$, 59296-75-2; PtOEP, 31248-39-2.

Ligand Design and Metal-Ion Recognition. Interaction of Nickel(II) with 17- to 19-Membered Macrocycles Containing O_2N_3 and O_3N_2 Donor Sets and the X-ray Structure of the Parent 17-Membered Macrocyclic Ligand

Kenneth R. Adam,[1a] Anthony J. Leong,[1a] Leonard F. Lindoy,*[1a] Hyacinth C. Lip,[1a] Brian W. Skelton,[1b] and Allan H. White[1b]

Contribution from the Department of Chemistry and Biochemistry, James Cook University, Queensland, 4811 Australia, and Chemistry Department, University of Western Australia, Nedlands, Western Australia, 6009 Australia. *Received October 12, 1982*

Abstract: A range of 17–19-membered macrocycles incorporating O_2N_3 and O_3N_2 donor sets has been synthesized and their interaction with nickel(II) studied. The X-ray structure of the parent 17-membered O_2N_3 ring indicates that the macrocyclic hole size is too large to enable simultaneous coordination of all donor atoms to nickel unless ligand folding occurs. An investigation of a selection of the nickel complexes in the solid state and in solution has been performed, and in all cases the results are consistent with the presence of either octahedral or pseudo-octahedral coordination geometries. In solution, the unsubstituted 17- and 18-membered O_2N_3 rings appear to adopt a configuration about nickel in which two oxygens and two nitrogens occupy equatorial positions while the remaining nitrogen coordinates at an axial site. The remaining axial position is occupied by a halide ion. In contrast, apparently as a consequence of steric crowding in the portion of the ligand backbone incorporating the three nitrogen donors, each of the 19-membered ring complexes are found to adopt a structure different from that of the above complexes. A similar structural "dislocation" can be induced by introduction of two methyl substituents onto the N_3-containing backbone of the unsubstituted 17-membered ring complex. The effects of such structural dislocations are most readily apparent in the stability constant variations observed across this series of complexes. The complexes postulated to undergo such dislocations give stability constants that are 10^3–10^5 lower than the remaining complexes. A comparison of the stability constants for the nickel complexes with those for the corresponding cobalt(II) complexes indicates that both series have similar "dislocation" patterns. In contrast, the complexes of copper(II) (for which the evidence suggests noncoordination of one or both ether oxygens in some complexes) exhibit a different stability pattern. The different behavior for copper, coupled with a knowledge of where dislocations occur for nickel and cobalt, makes possible the selection of reagents showing enhanced discrimination for copper over these other ions. More important, the study serves to illustrate the manner in which minor changes in macrocyclic ligand structure can be used to control alternate modes of ligand coordination—a process that can contribute to metal-ion recognition by organic substrates.

Introduction

An understanding of the factors underlying metal-ion recognition by organic substrates has wide-ranging ramifications for many areas of both chemistry and biochemistry. We have previously published accounts of the interaction of a number of transition- and post-transition-metal ions with a range of oxygen–nitrogen and sulfur–nitrogen donor macrocycles;[2-5] a principal aim of these studies has been to search for metal–ion discrimination and to understand the nature of such discrimination when it does occur. Mixed-donor complexes have proved especially suitable for such studies since they do not exhibit the large kinetic and thermodynamic stabilities that in some cases have made the solution study of related all-nitrogen donor systems somewhat difficult.[6]

Apart from the usual parameters influencing the affinities of open-chain ligands for particular ions (namely, variation of structural factors, donor-atom type, etc.), cyclic ligands can be further "tuned" by adjusting the macrocyclic hole size until an optimum fit for the metal ion of interest is achieved. Such use of macrocyclic hole-size variation to control the thermodynamic stabilities of metal complexes is of considerable current interest, and many studies of this type involving cyclic polyether ligand and non-transition-metal ions have been reported.[7] However, similar studies directed at achieving metal-ion specificity for particular transition ions have received less attention. In a previous investigation of this latter type, comparisons of the kinetic and thermodynamic stabilities of the nickel complexes of the 14–17-

(1) (a) James Cook University. (b) University of Western Australia.
(2) Armstrong, L. G.; Grimsley, P. G.; Lindoy, L. F.; Lip, H. C.; Norris, V. A.; Smith, R. J. *Inorg. Chem.* **1978**, *17*, 2350–2352. Ekstrom, A.; Lindoy, L. F.; Lip, H. C.; Smith, R. J.; Goodwin, H. J.; McPartlin, M.; Tasker, P. A. *J. Chem. Soc., Dalton Trans.* **1979**, 1027–1031. Adam, K. R.; Anderegg, G.; Lindoy, L. F.; Lip, H. C.; McPartlin, M.; Rea, J. H.; Smith, R. J.; Tasker, P. A. *Inorg. Chem.* **1980**, *19*, 2956–2964. Lindoy, L. F.; Lip, H. C.; Rea, J. H.; Smith, R. J.; Henrick, K.; McPartlin, M.; Tasker, P. A. *Ibid.* **1980**, *19*, 3360–3365. Lindoy, L. F.; Smith, R. J. *Ibid.* **1981**, *20*, 1314–1316.
(3) Anderegg, G.; Ekstrom, A.; Lindoy, L. F.; Smith, R. J. *J. Am. Chem. Soc.* **1980**, *102*, 2670–2674.
(4) Ekstrom, A.; Lindoy, L. F.; Smith, R. J. *Inorg. Chem.* **1980**, *19*, 724–727.
(5) Adam, K. R.; Lindoy, L. F.; Lip, H. C.; Rea, J. H.; Skelton, B. W.; White, A. H. *J. Chem. Soc., Dalton Trans.* **1981**, 74–79.
(6) Anichini, A.; Fabbrizzi, L.; Paoletti, P.; Clay, R. M. *J. Chem. Soc., Dalton Trans.* **1978**, 577–583. Hinz, F. P.; Margerum, D. W. *Inorg. Chem.* **1974**, *13*, 2941–2949. Tabushi, I.; Fujiyoshi, M. *Tetrahedron Lett.* **1978**, 2157–2160.
(7) Lehn, J. M. *Struct. Bonding (Berlin)* **1973**, *16*, 1–69. Christensen, J. J.; Eatough, D. J.; Izatt, R. M. *Chem. Rev.* **1974**, *74*, 351–384.

0002-7863/83/1505-4645$01.50/0

membered macrocycles of type **1** have been obtained.[3] Along this

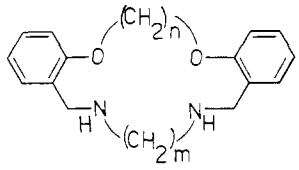

1; m = 2 or 3, n = 2, 3 or 4

ligand series, maximum kinetic and thermodynamic stability occurs at the 16-membered ring complex; in accordance with this, calculations based on X-ray structural data indicate that the fit of high-spin nickel for the 16-membered ring is near ideal.[8-10]

During the course of our studies so far, a second mechanism for macrocyclic hole-size discrimination has also been discerned.[11] Such discrimination involves the occurrence of a "dislocation" in the complexation behavior of a particular metal ion along a series of closely related ligands. Discrimination of this second type occurs, for example, when the gradation of properties along the ligand series triggers a change in coordination geometry for adjacent complexes at a particular point along the series. Because of their cyclic nature, macrocyclic ligands have inherent constraints that are expected to promote such dislocations. This type of macrocyclic ligand discrimination differs from the previously mentioned type since it is not necessarily dependent on the close fit of the metal ion for the macrocyclic hole. Discrimination may occur, for example, even when the macrocyclic ring sizes are considerably larger than are required to tightly surround the metal ion involved. A knowledge of where such dislocations occur within a ligand series for different metal ions is of practical use for choosing a ligand type to maximize the discrimination between particular ions of interest. A survey of the metal-ion chemistry of macrocyclic ligands in solution reveals many examples of apparent dislocation discrimination scattered throughout the literature. However, little emphasis has been given to a systematic study of this discrimination mechanism in the past. Apart from the implications for the design of a new metal-ion specific reagents, such studies may also contribute to a more general understanding of metal-ion recognition by organic substrates.

We now report the first of several studies designed to investigate ring-size discrimination of this latter type. In particular, the present work gives emphasis to a comparative study of the interaction of the 17–19-membered macrocycles (**2–10**, Chart I) with nickel (II).

Chart I

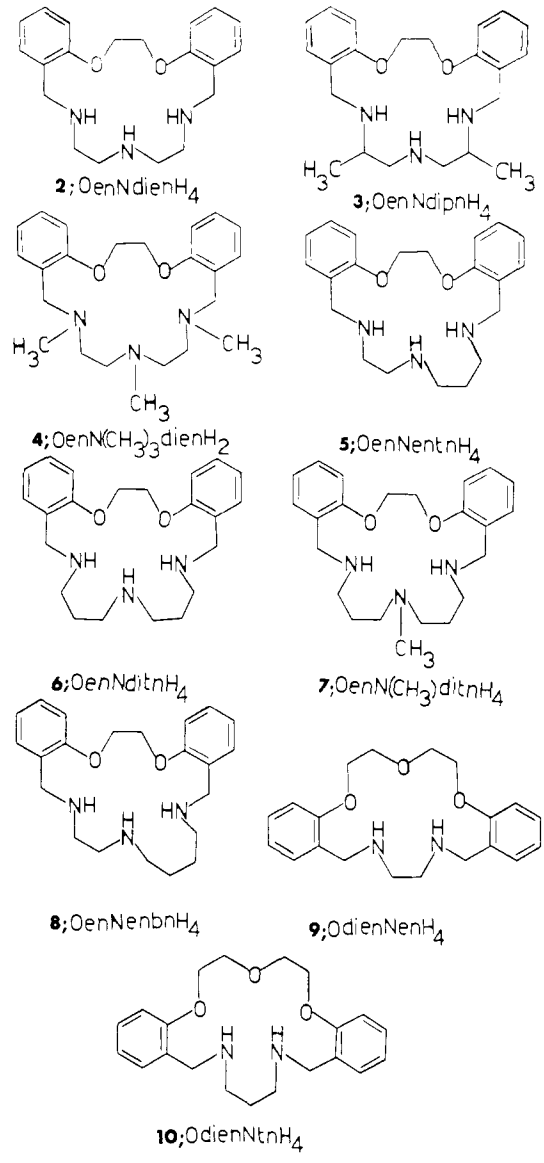

Experimental Section

Conductance, magnetic moment, infrared and visible spectrophotometric, NMR, mass spectra, and elemental analytical data were obtained as described previously.[2]

log *K* Determinations. The potentiometric cell, supporting electrolyte [0.1 M, $(CH_3)_4NCl$], purification of reagents, solvent system (95% methanol), and conditions of measurement were identical with those described previously.[3] An Exidy Sorcerer microcomputer was used to control the operation of the Metrohm automatic buret (Dosimat 655) as well as for data logging. The titration data were obtained in the form of millivolts vs. milliliters of base added and stored in the memory of the microcomputer as well as being displayed on a VDU. The amount of titrant added at each point was controlled by the microcomputer such that the voltage change between points remained less than 10 mV. The establishment of equilibrium at each point was also monitored by the microcomputer using appropriate default criteria (preset by the operator). In addition, the approach to equilibrium at each point was recorded independently by using a Varian Model 9176 recorder. On completion of a titration, the data were stored on a floppy disk [Micropolis (1040/1) disk drive] as well as transferred via a direct interface to the University's Digital DEC System 1091 computer for processing using local versions of the programs MINIQUAD[12] or KONST.[13] Titration curves were obtained in each case from data stored on the floppy disk and either displayed on the VDU or obtained as hard copy with the aid of a Houston Hiplot digital plotter interfaced to the microcomputer. Protonation constants for the respective ligands were determined separately and the values obtained used in the metal complex stability constant calculations. Solutions of the solid complexes in 95% methanol as well as mixtures of the corresponding free macrocycle and nickel ion dissolved in this solvent were both used for the stability constant determinations. In all, 105 potentiometric titrations were performed during the present investigation.

Ligand Synthesis. All compounds were dried over P_2O_5 in a vacuum. All melting points are uncorrected.

1,12,15-Triaza-3,4:9,10-dibenzo-5,8-dioxacycloheptadecane (OenNdienH$_4$, 2). The preparation and characterization of this macrocycle is described elsewhere;[5] mp 151 °C.

1,12,15-Triaza-3,4:9,10-dibenzo-13,17-dimethyl-5,8-dioxacycloheptadecane (OenNdipnH$_4$, 3). The preparation of this compound and its characterization are described elsewhere;[5] mp 185 °C.

1,12,15-Triaza-3,4:9,10-dibenzo-1,12,15-trimethyl-5,8-dioxacycloheptadecane Hydrate (OenN(CH$_3$)$_3$dienH$_2$·H$_2$O, 4). To OenNdienH$_4$ (5.0 g) was added excess 95% formic acid (32 mL). After the solid had dissolved, excess 40% formaldehyde solution (27 mL) was added, and the mixture was refluxed for 24 h. The resultant solution was chilled to 5 °C, and concentrated ammonia was added slowly (with stirring) to yield a final pH of 10. During the addition of ammonia the temperature did

(8) Tasker, P. A.; Trotter, J.; Lindoy, L. F. *J. Chem. Res., Miniprint* **1981**, 3834–3862.
(9) Goodwin, J. H.; Henrick, K.; Lindoy, L. F.; McPartlin, M.; Tasker, P. A. *Inorg. Chem.* **1982**, *21*, 3261.
(10) Drummond, L. A.; Henrick, K.; Kanagasundaram, M. J. L.; Lindoy, L. F.; McPartlin, M.; Tasker, P. A. *Inorg. Chem.* **1982**, *21*, 3923–3927.
(11) Leong, A. J.; Lindoy, L. F., unpublished work.
(12) Gans, P.; Sabatini, A.; Vacca, A. *Inorg. Chim. Acta* **1976**, *18*, 237–239.
(13) Anderegg, G. *Helv. Chim. Acta* **1961**, *44*, 1673–1690.

not rise above 15 °C. The product separated as a white solid. The product was filtered off, washed with water, dried, and then recrystallized from diethyl ether (very soluble); yield 2.3 g; mp 60 °C. Anal. Calcd for $C_{23}H_{33}N_3O_2 \cdot H_2O$: C, 68.8; H, 8.8; N, 10.5. found: C, 68.5; H, 8.7; N, 10.4. Mass spectral parent ion, m/e 383; ^{1}H NMR ($CDCl_3$) δ 2.15 (s, NCH_3, 3 H), 2.28 (s, NCH_3, 6 H), 5.28 (s, NCH_2CH_2N), 3.51 (s, Ar CH_2), 4.38 (s, OCH_2), 6.8–7.4 (m, Arom); ^{13}C NMR ($CDCl_3$) δ 43.5 (NCH_3), 54.6, 55.0, 55.9 (NCH_2), 66.8 (OCH_2), 111.3, 120.4, 127.3, 128.2, 131.7, 156.9, (Ar).

1,12,16-Triaza-3,4:9,10-dibenzo-5,8-dioxacyclooctadecane (OenNentnH$_4$, 5). This macrocycle was prepared as described elsewhere; mp 137 °C. Anal. Calcd for $C_{21}H_{29}N_3O_2$: C, 70.9; H, 8.2; N, 11.8. Found: C 70.6; H, 8.3; N, 11.7. ^{1}H and ^{13}C NMR spectra were identical with those reported previously.[5]

1,12,16-Triaza-3,4:9,10-dibenzo-5,8-dioxacyclononadecane Hemihydrate (OenNditnH$_4$·0.5H$_2$O, 6). In a manner similar to that described elsewhere,[5] bis(3-aminopropyl)amine (6.56 g; Pfaltz & Bauer) and 1,4-bis(2′-formylphenyl)-1,4-dioxabutane yielded the crude product as an oil that solidified on standing. The resulting solid was recrystallized from ether; however, ^{13}C NMR spectroscopy indicated that this product was slightly contaminated. Further purification was effected via the corresponding nickel complex. The above product was added to a slight excess of nickel chloride hexahydrate in hot 1:1 methanol/butanol. The solution was cooled and let stand at 0 °C, and the green nickel complex that precipitated was filtered off and recrystallized from boiling methanol. The resulting product was dissolved in a minimum amount of hot water (a small amount of nickel hydroxide formed, and this was removed by filtration), and then excess of disodium ethylenediaminetetraacetate was added to the blue solution. The solution was adjusted to pH 12 with sodium hydroxide, whereupon the free macrocycle began to separate as an oil. The solution was extracted (three times) with chloroform, and the chloroform extracts were combined and reduced to ~5 mL by using a rotary evaporator. Excess diethyl ether was added to the solution, which was allowed to stand at 0 °C; the required product separated as colorless crystals. The product was filtered off, washed with ether, and isolated as its hemihydrate; yield 4.0 g; mp 95 °C. Anal. Calcd for $C_{22}H_{31}N_3O_2 \cdot 0.5H_2O$: C, 69.8; H, 8.5; N, 11.1. Found: C, 70.1; H, 8.5; N, 11.0. Mass spectral parent ion, m/e 369; ^{1}H NMR ($CDCl_3$) δ 1.58 (quin, CCH_2C), 1.76 (s, NH), 2.59 (center of two overlapping triplets) ($CH_2CH_2CH_2$), 3.77 (s, Ar CH_2), 4.38 (s, OCH_2), 6.8–7.3 (m, Ar); ^{13}C NMR ($CDCl_3$) δ 29.1 (CCH_2C), 47.4, 47.5 ($CH_2CH_2CH_2$), 48.8 (Ar CH_2), 67.6 (OCH_2), 112.2, 121.0, 127.8, 129.6, 130.0, 156.7 (Ar).

1,12,16-Triaza-3,4:9,10-dibenzo-12-methyl-5,8-dioxacyclononadecane (OenN(CH$_3$)ditnH$_4$, 7). This was prepared from 3,3′-diamino-*N*-methyldipropylamine (3.00 g; Aldrich) and 1,4-bis(2′-formylphenyl)-1,4-dioxabutane (5.40 g) by the general method.[5] It was recrystallized from a chloroform/ether mixture; yield 2.32 g; mp 117 °C. Anal. Calcd for $C_{23}H_{33}N_3O_2$: C, 72.0; H, 8.7; N, 11.0. Found: C,, 71.5; H, 8.7; N, 10.9. Mass spectral parent ion, m/e 383; ^{1}H NMR ($CDCl_3$) δ 1.57 (quin, CCH_2C), 1.97 (s, NH), 2.14 (s, CH_3), 2.35, 2.68 (t, $CH_2CH_2CH_2$), 3.82 (s, Ar CH_2), 4.35 (s, OCH_2), 6.8–7.4 (m, Ar); ^{13}C NMR ($CDCl_3$) δ 26.9 (CCH_2C), 43.0 (NCH_3), 47.7, 48.6 (Ar CH_2NHCH_2), 55.2 ($CH_2N(CH_3)$), 67.2 (OCH_2), 111.6, 120.9, 127.8, 129.4, 129.6, 156.5 (Ar).

1,12,17-Triaza-3,4:9,10-Dibenzo-5,8-dioxacyclononadecane (OenNenbnH$_4$, 8). This was prepared from *N*-(2-aminoethyl)-1,4-butanediamine (2.38 g; Ames Laboratories) and 1,4-bis(2′-formylphenyl)-1,4-dioxabutane (5.40 g) by the general method.[5] It was recrystallized from an ether/methanol mixture; yield 1.10 g; mp 122 °C. Anal. Calcd for $C_{22}H_{31}N_3O_2$: C, 71.7; H, 8.2; N, 11.4. Found: C, 71.0; H, 8.5; N, 11.2. Mass spectral parent ion, m/e 369; ^{1}H NMR ($CDCl_3$) δ 1.49 (m, $CH_2CH_2CH_2CH_2$), 1.84 (br, NH), 2.57–2.72 (m, NCH_2CH_2), 3.82, (s, Ar CH_2), 4.38 (s, OCH_2), 5.8–7.3 (Ar); ^{13}C NMR ($CDCl_3$) δ 26.4 ($CH_2CH_2CH_2CH_2$), 47.8, 48.0, 48.9 (NCH_2CH_2; Ar CH_2), 67.1, 67.4 (OCH_2), 111.3, 111.8, 120.9, 128.0, 129.1, 129.2, 130.1, 156.7 (Ar).

1,7-Bis(2′-formylphenyl)-1,4,7-trioxaheptane $^1/_3$Hydrate (Odien·$^1/_3$H$_2$O). To salicylaldehyde (61.06 g) in dimethyl sulfoxide (100 mL) was added sodium hydroxide (20 g) in water (200 mL). To this was added 2,2′-dichloroethyl ether (35.75 g, Fluka) in dimethyl sulfoxide (100 mL). The solution was refluxed under nitrogen for 72 h then cooled to room temperature. Excess ice was slowly added to the stirred solution, and the product that formed was filtered off. The solution was then extracted with chloroform (three times), and the chloroform extract was reduced to 40 mL. On standing at 0 °C, further product precipitated. The dialdehyde was recrystallized from 80% methanol; yield 24 g; mp 73.5 °C; mass spectral parent ion, m/e 314. Anal. Calcd for $C_{18}H_{18}O_5 \cdot {}^1/_3H_2O$: C, 67.5; H, 5.9. Found: C, 67.3; H, 5.9. ^{1}H NMR ($CDCl_3$) δ 3.99, 4.24 (t, OCH_2), 7.0–7.8 (m, Ar); 10.52 (CHO); ^{13}C NMR ($CDCl_3$) δ 68.3, 69.8 (OCH_2), 112.8, 120.9, 125.0, 128.3, 135.8, 160.9 (Ar), 189.5 (CHO).

1,15-Diaza-3,4:12,13-dibenzo-5,8,11-trioxacycloheptadecane Hemihydrate (OdienNenH$_4$·0.5H$_2$O, 9). To Odien (3.1 g) in warm methanol (400 mL) was added ethylenediamine (0.6 g) in methanol (20 mL). The warm solution was stirred for 5 min, and then a small amount of borax followed by sodium borohydride (1.2 g) was slowly added to the stirred solution. The solution was then filtered, and water (200 mL) containing sodium carbonate (3 g) was slowly added to the filtrate. The volume was reduced to 250 mL by using a rotatory evaporator. The solution was extracted with chloroform (three times); the chloroform extracts were dried over anhydrous sodium sulfate and then evaporated to dryness to yield a crude oil. Ether (300 mL) was added to the oil, and the mixture was stirred and warmed slowly. Any undissolved solid was discarded. The solution was reduced to 20 mL and then let stand at 0 °C. Colorless crystals of hydrated product formed over 24 h. These were filtered off and washed sparingly with cold ether (product is quite soluble); yield 0.9 g; mp 97 °C. The water of hydration is slowly lost in air (original translucent crystals turn opaque on standing). When the above samples was dried for 3 h over P_2O_5 at 60 °C in a vacuum, a product containing half of a water molecule was obtained. Calcd for $C_{20}H_{26}N_2O_3 \cdot {}^1/_2H_2O$: C, 68.3; H, 7.7; N, 8.0. Found: C, 68.2; H, 7.8; N, 7.9. Mass spectral parent ion, m/e 342; ^{1}H NMR ($CDCl_3$) δ 2.21 (s, NH), 2.63 (s, NCH_2), 3.80 (s, Ar CH_2), 3.90, 4.20 (t, OCH_2), 6.8–7.3 (m, Ar); ^{13}C NMR ($CDCl_3$) δ 48.4 (NCH_2CH_2), 50.6 (Ar CH_2), 67.5, 69.9 (OCH_2), 111.8, 120.9, 128.4, 128.7, 130.8, 157.0 (Ar).

1,15-Diaza-3,4:12,13-dibenzo-5,8,11-trioxacyclooctadecane·$^1/_3$Hydrate (OdienNtnH$_4$·$^1/_3$H$_2$O, 10). To a stirred, warm solution of Odien (3.77 g) in methanol (400 mL) was slowly added propane-1,3-diamine (0.8 g) in methanol (20 mL). The solution was stirred for 5 min, and then sodium borohydride (2.5 g) together with a small amount of borax was slowly added to the stirred solution. After the reaction had ceased, the solution was cooled and then filtered. On addition of ice to the filtrate an oil separated, which was extracted into chloroform (three times). The extracts were dried over anhydrous sodium sulfate. The chloroform was removed by using a rotary evaporator to yield an oil that eventually crystallized to form a white solid. The product was recrystallized from ether; yield 2.0 g; mp 84 °C. Anal. Calcd for $C_{21}H_{28}N_2O_3 \cdot {}^1/_3H_2O$: C, 69.6; H, 8.0; N, 7.7. Found: C, 69.6; H, 8.0; N, 7.8. Mass spectral parent peak, m/e 356; IR ν(OH) 3360 cm^{-1} (br); ^{1}H NMR ($CDCl_3$) δ 1.69 (quin, CCH_2C), 2.11 (s, NH), 2.67, (t, NCH_2CH_2), 3.81 (s, Ar CH_2), 3.95, 4.14, m (OCH_2CH_2), 5.7–7.3 (m, Ar); ^{13}C NMR ($CDCl_3$) δ 29.1 (CCH_2C), 46.6, 49.2, 49.9 (Ar CH_2NHCH_2), 67.9, 70.2 (OCH_2), 111.4, 120.9, 128.3, 128.5, 130.6, 156.9 (Ar).

Synthesis of the Complexes. Type Ni(macrocycle)X$_2$·*n*solvate (X = Cl, Br, or ClO$_4$). Macrocycle (0.001 mol) in hot methanol or butanol was added dropwise to a stirred boiling solution of the required metal salt (0.001 mol) in methanol, butanol or a mixture of these solvents. The complex that precipitated was filtered off (in some cases it was necessary to concentrate the solution first) and was washed with methanol or butanol. It was dried in a vacuum over P_2O_5; yields 40–80%.

[Ni(OenNdienH$_4$)Cl]ClO$_4$. To [Ni(OenNdienH$_4$)](ClO$_4$)$_2$ (0.001 mol) suspended in refluxing methanol (50 mL) was added lithium chloride (0.001 mol) in methanol (20 mL). The reaction mixture was heated at the reflux and then filtered and let stand at room temperature. Blue microcrystals of product formed; these were washed with methanol and dried in a vacuum over P_2O_5; yield 60%.

Analytical data for the complexes are given in the supplementary data (Table SUP-1).

Crystallography. An X-ray structural determination of the parent free ligand in the O_2N_3 donor series, **2**, has been carried out.

Crystal Data: $C_{20}H_{27}N_3O_2$, M_r 341.5, triclinic, space group $P\bar{1}$ (C_i^1, No. 2) a = 11.142 (3) Å, b = 10.282 (3) Å, c = 8.818 (2) Å, α = 75.32 (2)°, β = 82.26 (2)°, γ = 71.78 (2)°, U = 926.5 (5) Å^3, D_m = 1.21 (1), D_c (Z = 2) = 1.22 g cm^{-3}, F(000) = 368, T = 295 (1) K, μ(Mo Kα) = 0.85 cm^{-1}.

Structure Determination. A unique data set was measured, using a well-formed prismatic crystal ca. 0.4 mm on edge, with a Syntex P2$_1$ four-circle diffractometer in conventional $2\theta/\theta$ scan mode, the $2\theta_{max}$ limit being 60°. A total of 5456 independent reflections were obtained, 3449 of these with $I > 3\sigma(I)$ being used in the (basically) 9 × 9 block diagonal least-squares refinement without absorption correction and after solution of the structure by direct methods. x,y,z for all atoms were refined, together with anisotropic thermal parameters for the non-hydrogen atoms and isotropic for the hydrogens; hydrogen atom parameters were included in the block of the parent atom. Residuals (R, R') at convergence were 0.044, 0.058, reflection weights being $(\sigma^2(F_o) + 0.0005(F_o)^2)^{-1}$. Neutral atom scattering factors were used, those for the non-hydrogen atoms being corrected for anomalous dispersion (f', f'').[14] Computation used

(14) "International Tables for X-ray Crystallography"; Ibers, J. A., Hamilton, W. C., Eds.; Kynoch Press: Birmingham, England, 1974; Vol. IV.

Table I. Atom Coordinates for OenNdienH$_4$

atom	x	y	z
N(1)	0.6055 (1)	0.1089 (1)	0.3507 (1)
H(1)	0.525 (2)	0.162 (2)	0.364 (2)
C(2)	0.6914 (2)	0.1926 (2)	0.3427 (2)
H(2A)	0.688 (1)	0.211 (2)	0.449 (2)
H(2B)	0.777 (2)	0.131 (2)	0.325 (2)
C(3)	0.6699 (1)	0.3315 (1)	0.2223 (2)
C(31)	0.7630 (2)	0.3575 (2)	0.1069 (2)
H(31)	0.838 (2)	0.286 (2)	0.099 (2)
C(32)	0.7481 (2)	0.4893 (2)	0.0062 (2)
H(32)	0.818 (2)	0.501 (2)	−0.071 (2)
C(33)	0.6394 (2)	0.5949 (2)	0.0185 (2)
H(33)	0.631 (2)	0.686 (2)	−0.050 (2)
C(34)	0.5433 (2)	0.5729 (2)	0.1308 (2)
H(34)	0.467 (2)	0.648 (2)	0.140 (2)
C(4)	0.5592 (1)	0.4413 (1)	0.2317 (2)
O(5)	0.4707 (1)	0.4091 (1)	0.3484 (1)
C(6)	0.3621 (1)	0.5198 (2)	0.3793 (2)
H(6A)	0.392 (1)	0.591 (2)	0.403 (2)
H(6B)	0.309 (2)	0.556 (2)	0.289 (2)
C(7)	0.2879 (1)	0.4596 (2)	0.5184 (2)
H(7A)	0.345 (1)	0.395 (2)	0.593 (2)
H(7B)	0.229 (2)	0.536 (2)	0.565 (2)
O(8)	0.2161 (1)	0.3878 (1)	0.4675 (1)
C(9)	0.1395 (1)	0.3255 (1)	0.5790 (2)
C(91)	0.1449 (2)	0.3074 (1)	0.7399 (2)
H(91)	0.204 (2)	0.334 (2)	0.777 (2)
C(92)	0.0651 (2)	0.2413 (2)	0.8433 (2)
H(92)	0.066 (2)	0.232 (2)	0.951 (2)
C(93)	−0.0192 (2)	0.1945 (2)	0.7868 (2)
H(93)	−0.073 (2)	0.145 (2)	0.863 (2)
C(94)	−0.0255 (2)	0.2153 (2)	0.6268 (2)
H(94)	−0.082 (2)	0.186 (2)	0.586 (2)
C(10)	0.0524 (1)	0.2818 (1)	0.5190 (2)
C(11)	0.0418 (1)	0.3110 (2)	0.3437 (2)
H(11A)	−0.037 (2)	0.292 (2)	0.324 (2)
H(11B)	0.030 (1)	0.416 (2)	0.298 (2)
N(12)	0.1477 (1)	0.2329 (1)	0.2545 (1)
H(12)	0.218 (2)	0.244 (2)	0.275 (2)
C(13)	0.1687 (2)	0.0816 (2)	0.2970 (2)
H(13A)	0.166 (2)	0.045 (2)	0.410 (2)
H(13B)	0.098 (2)	0.060 (2)	0.259 (2)
C(14)	0.2946 (2)	0.0062 (2)	0.2269 (2)
H(14A)	0.307 (2)	−0.097 (2)	0.247 (2)
H(14B)	0.295 (2)	0.036 (2)	0.113 (2)
N(15)	0.3958 (1)	0.0398 (1)	0.2825 (2)
H(15)	0.390 (2)	0.019 (2)	0.384 (2)
C(16)	0.5244 (2)	−0.0369 (2)	0.2357 (2)
H(16A)	0.558 (2)	−0.123 (2)	0.314 (2)
H(16B)	0.523 (2)	−0.066 (2)	0.141 (2)
C(17)	0.6130 (2)	0.0542 (2)	0.2111 (2)
H(17A)	0.700 (2)	−0.002 (2)	0.195 (2)
H(17B)	0.589 (2)	0.136 (2)	0.118 (2)

the X-ray program system implemented by S. R. Hall on a Perkin-Elmer 3240 computer.[15] Non-hydrogen atom labeling is given in Figure 1; hydrogen atom labeling follows that of the parent atom, with suffixes A and B for distinguishing purposes. Atom coordinates are given in Table I.

Results and Discussion

An important aspect of the present work has been the synthesis of the range of cyclic ligands **2–10**. Taken together, these ligands provided a matrix of structural types against which the search for dislocation discrimination was based. Although emphasis is usually given to solution measurements in such studies, it has been our experience that metal-ion discrimination effects are almost invariably better understood when a broad investigation of the chemistry of the macrocyclic system of interest is undertaken simultaneously. Accordingly, the synthesis and characterization of a number of solid nickel complexes of selected macrocycles in the series as well as an X-ray diffraction study of the structure

(15) "The X-Ray System"; Report TR-446; Computer Science Center, University of Maryland, MD, March 1976.

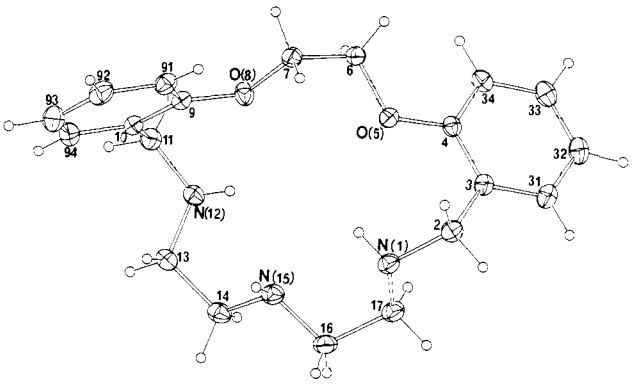

Figure 1. Single molecule of OenNdienH$_4$. Hydrogen atoms are shown as circles of arbitrary radius 0.1 Å. The thermal ellipsoids given are at the 20% probability level.

Table II. Molecular Non-Hydrogen Geometries

atoms	parameter	atoms	parameter
	Distances (Å)		
N(1)–C(2)	1.459 (3)	C(11)–N(12)	1.461 (2)
C(2)–C(3)	1.520 (2)	C(10)–C(11)	1.512 (2)
C(3)–C(4)	1.397 (2)	C(9)–C(10)	1.398 (3)
C(3)–C(31)	1.392 (2)	C(94)–C(10)	1.393 (2)
C(31)–C(32)	1.393 (2)	C(93)–C(94)	1.380 (3)
C(32)–C(33)	1.364 (2)	C(92)–C(93)	1.376 (3)
C(33)–C(34)	1.389 (2)	C(91)–C(92)	1.388 (3)
C(34)–C(4)	1.391 (2)	C(9)–C(91)	1.391 (2)
C(4)–O(5)	1.378 (2)	O(8)–C(9)	1.379 (2)
O(5)–C(6)	1.429 (2)	C(7)–O(8)	1.422 (3)
C(6)–C(7)	1.494 (2)		
N(1)–C(17)	1.461 (2)	C(13)–N(12)	1.454 (2)
C(17)–C(16)	1.522 (3)	C(14)–C(13)	1.510 (2)
C(16)–N(15)	1.465 (2)	N(15)–C(14)	1.452 (3)
	Angles (deg)		
C(14)–N(15)–C(16)	115.5 (1)		
N(15)–C(16)–C(17)	110.8 (1)	N(15)–C(14)–C(13)	109.6 (2)
C(16)–C(17)–N(1)	109.8 (1)	C(14)–C(13)–N(12)	110.9 (1)
C(17)–N(1)–C(2)	114.4 (1)	C(13)–N(12)–C(11)	114.1 (1)
N(1)–C(2)–C(3)	118.2 (1)	N(12)–C(11)–C(10)	116.8 (1)
C(2)–C(3)–C(4)	120.8 (1)	C(11)–C(10)–C(9)	120.4 (1)
C(2)–C(3)–C(31)	121.4 (1)	C(11)–C(10)–C(94)	122.2 (2)
C(4)–C(3)–C(31)	117.7 (1)	C(9)–C(10)–C(94)	117.4 (2)
C(3)–C(31)–C(32)	121.4 (1)	C(10)–C(94)–C(93)	121.9 (2)
C(31)–C(32)–C(33)	119.7 (2)	C(94)–C(93)–C(92)	119.7 (2)
C(32)–C(33)–C(34)	120.8 (1)	C(93)–C(92)–C(91)	120.2 (2)
C(33)–C(34)–C(4)	119.2 (1)	C(92)–C(91)–C(9)	119.7 (2)
C(34)–C(4)–O(5)	123.8 (1)	C(91)–C(9)–O(8)	123.9 (2)
C(34)–C(4)–C(3)	121.3 (1)	C(91)–C(9)–C(10)	121.1 (1)
C(3)–C(4)–O(5)	114.9 (1)	O(8)–C(9)–C(10)	115.1 (1)
C(4)–O(5)–C(6)	118.6 (1)	C(9)–O(8)–C(7)	117.5 (1)
O(5)–C(6)–C(7)	107.7 (1)	O(8)–C(7)–C(6)	108.5 (1)

of the parent 17-membered ring macrocycle have been undertaken.

X-ray Diffraction Study. The X-ray structure of OenNdienH$_4$ indicates that it exists in a nonfolded configuration (Figure 1). The unit-cell contents comprise a pair of discrete centrosymmetrically related molecules of the macrocycle (**2**). The precision of the determination is good, and given the potential *2* or *m* symmetry of the system, the agreement between similar bonding parameters is also good, the maximum difference in similar bond lengths being 0.013 Å (Table II) and for similar angles 1.4°. In consequence, a number of variations within the system may be considered significant. Among the bond lengths, significant differences are observed between the aliphatic and aromatic C–O(ether) bonds, while among the bond angles, the asymmetry in the fusion of the ether oxygens at the phenyl rings is notable, as are the unusually large values of the angles at C(2,12) adjacent to the phenyl rings. Among the torsion angles within the macrocycle, a notable discrepancy between potentially equivalent values is found on either side of N(15) (Table III). A least-squares plane defined by the macrocycle has σ(defining atoms)

Table III. Torsion Angles (deg) in the Macrocycle[a]

atoms	angle	atoms	angle
14-15-16-17	146.7	16-15-14-13	174.4
15-16-17-1	53.5	15-14-13-12	59.1
16-17-1-2	177.3	14-13-12-11	−167.7
17-1-2-3	65.8	13-12-11-10	62.9
1-2-3-4	63.9	12-11-10-9	69.9
2-3-4-5	−4.7	11-10-9-8	−3.4
3-4-5-6	172.1	10-9-8-7	167.5
4-5-6-7	−175.3	9-8-7-6	−179.3
5-6-7-8	−79.6		

[a] Atoms are designated by number only.

0.66 Å, with maximum deviations to either side of the plane of 1.10 and 1.03 Å.

In recent publications, a general procedure for approximating the hole sizes of macrocyclic ligands has been outlined.[9,10] The procedure involves using X-ray data to obtain the mean distance of the donor atoms from their centroid followed by calculation of the radius of the "apparent" hole size available to the metal ion by correction of the above value for the mean radii of the donor atoms present. The radii of the respective donor atoms for both ether oxygen to high-spin nickel and secondary amine to high-spin nickel were estimated from crystallographic bond lengths by using data in the Cambridge Crystallographic Data Base.[9,10]

Macrocycle conformational changes would need to occur in the present case before coordination of all five donors to a metal ion could occur since N(1) and N(2) lie with their associated hydrogen atoms directed toward the centroid and distant 1.70 and 1.80 Å from it, respectively. This arrangement is presumably a consequence of both intramolecular [H(1)···O(5),N(15), 2.39 (2), 2.46 (2); H(12)···O(8), 2.51 (2); H(15)···N(1), 2.78 (2) Å] and intermolecular [H(15)···N(1) $(1-x, \bar{y}, 1-z)$, 2.37 (2) Å] hydrogen bonds.

Nevertheless rotation of the nitrogen atoms so that the attached hydrogens are exo to the ring should give a configuration of similar hole size with all potential donor atoms approximately aligned for coordination to a central metal ion. Thus applying the above procedure to the structure as found yields an apparent macrocyclic cavity of radius of 1.68 Å.[16] This radius is much larger than the Pauling radius for high-spin nickel of 1.39 Å. From the calculation it is clear that coordination of all donor atoms of the macrocycle to a central nickel ion will be unfavorable if the ligand maintains a nonfolded configuration. This conclusion is supported by inspection of a space-filling model of the molecule as well as by our previous studies involving related O_2N_2 macrocycles.[9,10] In these latter studies both the 15- and 16-membered macrocycles were found to present cavities that were near ideal for high-spin nickel.

Characterization of the Metal Complexes. Reaction of a selection of the O_2N_3 donor macrocycles with the corresponding nickel salts has led to the isolation of the following complexes: $Ni(OenNdienH_4)(ClO_4)_2$, $[Ni(OenNdienH_4)Cl](ClO_4)$, $[Ni(OenNdienH_4)Cl_2]\cdot 0.5BuOH$, $[Ni(OenNdienH_4)Br_2]\cdot 0.5BuOH$, $[Ni(OenNentnH_4)Cl_2]$, $[Ni(OenNditnH_4)Cl_2]\cdot H_2O$, and $[Ni(OenN(CH_3)_3dienH_2)Cl_2]\cdot H_2O$. Physical data for the complexes are summarized in supplementary Table SUP-6. The infrared spectra of the complexes confirmed the presence of solvent where it was suggested to be present from the analytical data. The visible–near infrared spectra are consistent with each of the complexes having either an octahedral or distorted octahedral geometry; the magnetic moments all fall in the normal range expected for complexes of high-spin nickel.

The nickel perchlorate complex of $OenNdienH_4$ gives a conductance value in methanol that indicates that both perchlorate groups are ionized in this solvent. The infrared spectrum of the solid complex gives no firm indication as to whether perchlorate coordination occurs in the solid state (no clear splitting or the perchlorate modes was observed). Nevertheless it seems likely that at least one perchlorate group does coordinate to give an overall pseudooctahedral geometry. Indeed, reaction of **2** with nickel perchlorate in the presence of chloride ion leads to isolation of the mixed anion complex, $[Ni(OenNdienH_4)Cl]ClO_4$, which is a 1:1 electrolyte in methanol. With the assumption of 6-coordination (as suggested by the electronic spectrum), inclusion of only one chloride ion into the coordination sphere implies that all heteroatoms of the macrocycle coordinate to the nickel ion. Further a conductimetric titration of $Ni(OenNdienH_4)(ClO_4)_2$ with tetramethylammonium chloride in methanol gave a weak inflection corresponding to a 1:1 end point, suggesting that the structure proposed for $[Ni(OenNdienH_4)Cl]^+$ in the solid state persists in solution. The visible spectra of $[Ni(OenNdienH_4)Cl]ClO_4$ in the solid (375, 610, 1020 nm) and in methanol (380, 625, 1030 nm) are similar. Moreover both spectra are also similar to that of $[Ni(OenNdienH_4)Cl_2]$ in methanol (Figure 2) but differ from the solid-state spectrum of this latter complex (395, 640, 1090 nm). This difference is most readily explained in terms of different structures for $[Ni(OenNdienH_4)Cl_2]$ in the solid and in solution. In the absence of X-ray structural data for this complex it is difficult to assign its solid-state structure, but it may well involve coordination of both chloride ions to the nickel. Similarly, the remaining complexes containing two chloride or bromide ions are all 1:1 electrolytes in methanol and are assigned octahedral or pseudooctahedral geometries in this solvent.

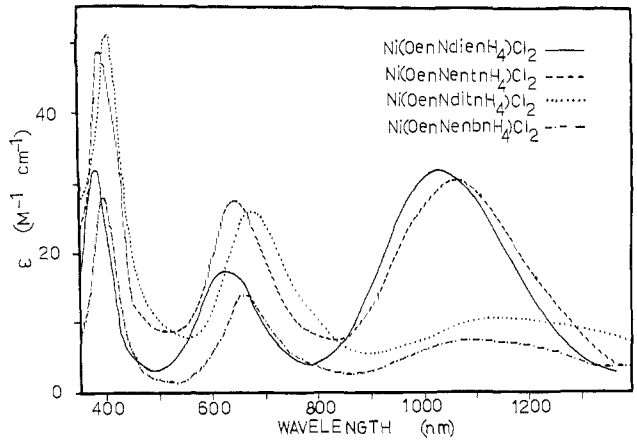

Figure 2. Electronic spectra for the complexes shown in absolute methanol.

It is of significance to the present work to compare the solution spectra (Figure 2) of the nickel chloride complexes of the 17–19-membered (unsubstituted) macrocycles **2**, **5**, and **6**. The spectra of the 17- and 18-membered ring complexes are very similar and show three transitions ($^3A_{2g} \rightarrow {}^3T_{1g}(P)$, $^3A_{2g} \rightarrow {}^3T_{1g}(F)$, $^3A_{2g} \rightarrow {}^3T_{2g}$) typical of effective octahedral symmetry. The energy of the $^3A_{2g} \rightarrow {}^3T_{2g}$ transition gives the $10Dq$ value directly; thus the 18-membered ring complex has a slightly lower ligand field than its 17-membered ring analogue—this is probably a reflection of the presence of an additional 6-membered chelate ring in this latter complex. In contrast, the spectra of the 19-membered ring complexes are clearly different and, although still consistent with a pseudooctahedral stereochemistry, strongly suggest that a variation in the coordination shell has occurred relative to the other two complexes in the series. The nature of this variation is discussed in the following section.

Stability Constant Studies. As mentioned previously, a successful strategy for observing dislocation discrimination has been to investigate complexation across a matrix of ligand types. Accordingly, potentiometric (pH) titrations have been carried out to determine the protonation constants for the macrocyclic ligands **2**–**10** as well as the stabilities of the corresponding 1:1 complexes with nickel (Table IV). The complexes of the unsubstituted 17–19-membered rings **2**, **5**, **6**, and **8** will be considered first. For the 17- and 18-membered ring complexes the log K values are very similar, with the larger ring showing only a slight drop in the observed constant. However, on passing to the two 19-mem-

(16) The centroid of the potentially coordinating atoms lies at (0.3672, 0.2357, 0.3407) and at distances of 2.57, 2.43, 2.29, 2.67, and 2.12 Å from N(1), O(5), O(8), N(12), and N(15), respectively. The radii of the nitrogen and oxygen donors used in the calculations were 0.72 and 0.76 Å, respectively.

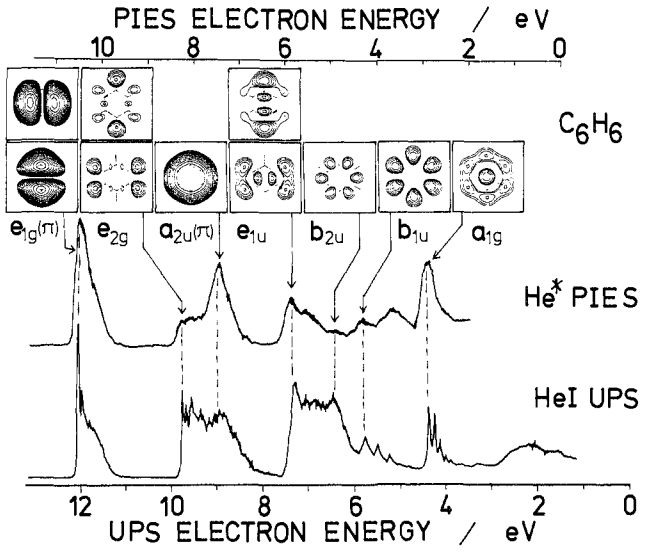

Figure 10. Transmission-corrected He*(2^3S) PIES (upper) and He I UPS (lower) for C_6H_6, and electron density maps for MO. The maps are drawn for a plane 1.7 Å above the molecular plane.

skeleton and shielded by the π orbitals, and therefore it is almost completely inactive in PIES.

More quantitative comparison between theory and experiment can be made for the orbital activities (α_{calcd} and α_{obsd}) listed in Table I. In general, the agreement between α_{calcd} and α_{obsd} is satisfactory. This means that the orbital selection in Penning ionization is governed by the exterior electron density of the relevant molecular orbital. It must be noted that only 1–10% of the orbital electron density (ρ = 0.01–0.10) governs the orbital activity in Penning ionization. This is a quite natural result of the reaction mechanism; the metastable atom, which behaves as an electrophilic reagent, attacks the frontier of the molecule and mainly interacts with "exterior electrons" spreading out from the molecular surface, which protects large numbers of "interior electrons" from the electrophilic attacks. In the case of photoionization, the molecular surface does not act as a repulsive wall to photons, which penetrate into the inside to interact also with the interior electrons.

We must make here some comments on the results in Table I. The relative activities of the π orbitals in N_2 and CO are more emphasized in the calculations; exterior electron densities for the σ orbitals, which are nonbonding or less bonding, are relatively underestimated. This may be due to the inaccuracy involved in the ab initio orbital functions; Weigold et al. pointed out on the basis of (e,2e) electron spectroscopy that usual ab initio calculations underestimate orbital electron densities at long range, especially for lone-pair-type (nonbonding) orbitals.[8] The values of α_{calcd} for the $1b_2$ orbital of H_2O and the $2b_2$ orbital of H_2S are rather large. This can be improved when the additional electron densities due to the unreal dips in the approximate molecular surface shown in Figures 5 and 6 are disregarded. Another discrepancy between α_{obsd} and α_{calcd} is found for H_2O. The calculation shows that the $1b_1$ orbital is more active than the $3a_1$ orbital, whereas the experimental activity of the $3a_1$ orbital is much larger than that of the $1b_1$ orbital. Since the underestimation of exterior electron density has been reported for the $1b_1$ orbital,[8] this discrepancy may be ascribed to other causes: (i) the crude approximation for the repulsive molecular surface or (ii) the anisotropic effect on the effective solid angle open to incoming metastable atoms. This latter effect has been found to be important for molecules in which steric shielding effects of some bulky groups are involved.[17,18]

In connection with the frontier electron theory by Fukui et al.,[39] a few comments must be made. Although highest occupied molecular orbitals (HOMO) are mostly active in the PIES of the molecules studied in the present work, the PIES activity is not necessarily concentrated on HOMO. The $2\sigma_u$ orbital of N_2 is more active in PIES than the $3\sigma_g$ and $1\pi_u$ orbitals. In the case of ferrocene,[17] the HOMO, which is due to iron d orbitals, has been found to be inactive in PIES. The π orbitals other than the HOMO are also very active in PIES for various aromatic molecules including naphthalene and anthracene.[12-16] These results can commonly be explained in terms of "exterior electrons" outside the repulsive molecular surface on the basis of the present model. It must be stressed here that the HOMO, which has been considered to be occupied by the "frontier electrons",[39] does not necessarily have the largest exterior electron density. Furthermore, the proximity condition for energies of the orbitals involved in the electron-transfer process is not important in Penning ionization, since the energy of the 1s orbital of a He atom is about −24.6 eV and much smaller than the orbital energies of relevant molecular orbitals. The decisive factor governing the electrophilic process in Penning ionization is not the proximity in energy but the proximity in real coordinate space between the inner-shell orbital of the metastable atom and the MO of the target molecule.

Table I. Exterior Electron Density (EED, ρ)[a] and Relative Orbital Activity (OA, α)[b]

		ρ_{calcd}[c]	α_{obsd} (α_{calcd})
NH_3	$3a_1$	0.050	1.00 (1.00)
	1e	0.031	0.39 (0.61)
H_2O	$1b_1$	0.037	0.61 (1.23)
	$3a_1$	0.030	1.00 (1.00)
	$1b_2$	0.022	0.48[d] (0.72)
H_2S	$2b_1$	0.053	1.00 (1.00)
	$5a_1$	0.045	0.70 (0.84)
	$2b_2$	0.044	0.44 (0.83)
N_2	$3\sigma_g$	0.030, 0.029	0.90 (1.23)
	$1\pi_u$	0.040, 0.025	0.36 (1.06)
	$2\sigma_u$	0.025, 0.023	1.00 (1.00)
CO	5σ	0.030, 0.030	1.00 (1.00)
	1π	0.028, 0.016	0.20 (0.53)
	4σ	0.018, 0.015	0.43[d] (0.50)
C_2H_2	$1\pi_u$	0.041	1.00 (1.00)
	$3\sigma_g$	0.021	0.51 (0.52)
	$2\sigma_u$	0.021	0.68[d] (0.52)

[a] The EED (ρ) is defined for each MO by the total electron densities outside the repulsive molecular surface. [b] The observed OA (α_{obsd}) is the relative PIES intensity for each MO. The calculated OA (α_{calcd}) is the relative value of the EED (ρ). The values of α are normalized to the value for the most active MO. [c] For simple diatomic molecules, N_2 and CO, the values for van der Waals surfaces (left) and those for more real surfaces (right) were calculated. These surfaces are shown by solid and dashed curves, respectively, in Figures 7 and 8. [d] A background subtracting technique was used and the vibrational contributions expected outside of the spectral range were estimated from the vibrational structures in the UPS.

In the present experiments, sample molecules are randomly oriented with respect to the metastable atom beam, and various parts of the molecular surface are probed on the average by the metastable atoms. When the direction of collision between metastable atoms and target molecules is controlled, for example, by introducing metastable atom beams with a definite direction onto a regular array of molecules adsorbed on a solid surface, the orbital electron density may be probed for a given part of the molecular surface. The variation of the orbital electron density along the direction vertical to the molecular surface can also be observed by controlling the relative velocity between the projectile and the target.

Conclusion

The nature of Penning ionization of closed-shell molecules induced by collision with metastable atoms can be understood as an electrophilic reaction in which an electron in a molecular orbital is transferred into the vacant orbital of the metastable atom. The orbital selection upon Penning ionization depends on the spatial electron distribution of the individual molecular orbital. It is of great note that the orbital activity in Penning ionization is governed

(39) Fukui, K.; Yonezawa, T.; Shingu, H. *J. Chem. Phys.* **1952**, *20*, 722–725.

speculate further concerning the structures of these complexes; it is emphasized that the discussion here is concerned with structures in solution that, as discussed earlier, may differ from the corresponding solid-state structures.

Comparison with Cobalt(II) and Copper(II). Table V lists stability constants for the cobalt(II) and copper(II) complexes of a selection of the O_2N_3 donor macrocycles. For the 1:1 metal:ligand complexes, the stability follows the expected Irving–Williams order (Co < Ni < Cu)[21] for each ring system. Apart from these 1:1 complexes, complexes of stoichiometry MLH were also detected in most cases. For the 1:1 complexes of cobalt, trends similar to those observed for nickel (Table IV) were observed. Namely, the stability constants for the dimethyl derivative $OenNdipnH_4$ (**3**) and for the two 19-membered rings (**6** and **8**) all show dislocations relative to the values obtained with the unsubstituted 17- and 18-membered rings **2** and **5**. Since identical stability patterns occur for both the nickel and cobalt series, it appears likely that the origins of the observed dislocations are similar for both these ions.

The interaction of this ligand series with copper(II) does not fully parallel the behavior with nickel(II) or cobalt(II). In particular, the dimethylated ligand **3** gives a stability constant for the 1:1 copper complex that is almost identical with that for the parent macrocycle—no dislocation of the type observed for the corresponding nickel or cobalt complexes occurs in this case. This difference is readily rationalized in terms of the previously postulated solution structures for the copper complexes of **2**, **3**, and **5**.[5] On the basis of the results of physical measurements taken together with the X-ray structural determination of $[Cu(OenNentnH_4)(H_2O)](ClO_4)_2$ (in which the macrocycle coordinates to the copper ion solely via its three nitrogen donors),[5] it was postulated that noncoordination of one or both ether oxygens occurs in these three complexes. As a consequence, dislocation effects might be expected either to be absent or to occur less frequently.

The different observed behavior of **3** with copper and nickel (or cobalt) results in enhanced discrimination for copper in the presence of these other ions. Thus the parent 17-membered macrocycle **2** forms a 1:1 copper complex whose stability constant is $10^{4.4}$ greater than that for nickel, whereas the corresponding dimethylated derivative **3** yields a stability difference of $10^{7.4}$ between these ions. This latter ring system also exhibits increased discrimination for copper over cobalt although, in this case, the effect is somewhat less marked (Table V).

The two 19-membered rings (**6** and **8**) again yield 1:1 species with copper that have lowered stability constants, but in the absence of structural data, it is inappropriate to speculate concerning the reasons for this.

(21) Irving, H.; Williams, R. J. P. *J. Chem. Soc.* **1953**, 3192–3210.

Concluding Remarks

The present study serves to illustrate that minor changes in macrocyclic ligand structure can be used to control alternate modes of ligand coordination to a particular metal ion. For such ligand systems, observation of different behavior toward different metal ions may form a basis for discriminating these ions. Further, an understanding of the subtle factors underlying such discrimination provides additional background for the design of new reagents having predetermined properties. The development of such reagents has implications for a number of areas. These include hydrometallurgy (solvent extraction of metals from leach solutions), the synthesis of new chromatography materials for separation of metal ions (macrocycles bonded to polymeric supports), and the development of selective reagents for use in a wide range of analytical, industrial, and medical applications.

Acknowledgment. L.F.L. and A.H.W. thank the Australian Research Grants Scheme for support of this work. L.F.L. also acknowledges the Australian Institute of Nuclear Science and Engineering for a travel grant. We thank Dr. R. J. Smith and B. Harrison for experimental assistance.

Registry No. 2, 77016-63-8; **4**, 85735-80-4; **6**, 85735-81-5; **7**, 85735-82-6; **8**, 85735-83-7; **9**, 85735-84-8; **10**, 85735-85-9; $Ni(OenNdienH_4)(ClO_4)_2$, 85735-88-2; $[Ni(OenNdienH_4)Cl]ClO_4$, 85735-90-6; $[Ni(OenNdienH_4)Cl_2]$, 85735-91-7; $[Ni(OenNdienH_4)Br_2]$, 85735-92-8; $[Ni(OenNentnH_4)Cl_2]$, 85735-93-9; $[Ni(OenNditnH_4)Cl_2]$, 85735-94-0; $[Ni(OenN(CH_3)_3dienH_2)Cl_2]$, 85748-33-0; $Ni(OenNenbnH_4)Cl_2$, 85735-95-1; Odien, 82645-24-7; formaldehyde, 50-00-0; bis(3-aminopropyl)amine, 56-18-8; 1,4-bis(2′-formylphenyl)-1,4-dioxabutane, 52118-10-2; 3,3′-diamino-*N*-methyldipropylamine, 105-83-9; *N*-(2-aminoethyl)-1,4-butanediamine, 35513-87-2; salicylaldehyde, 90-02-8; 2,2′-dichloroethyl ether, 111-44-4; ethylenediamine, 107-15-3; propane-1,3-diamine, 109-76-2.

Supplementary Material Available: Figure SUP-1 showing the contents of the unit cell for $OenNdienH_4$ and Tables SUP-1 (microanalyses), SUP-2 (thermal parameters), SUP-3 (hydrogen atom geometries), SUP-4 (least-squares planes), SUP-5 (structure factors), and SUP-6 (physical data for the solid complexes) (22 pages). Ordering information is given on any current masthead page.